Supporting Information

Iida et al. 10.1073/pnas.1311480111

SI Note 1: Importance of Histone Methylation During Retinal Development Suggested in Previous Studies

Genome-wide profiling of dimethylation of lysine 4 on histone H3 (H3K4me2) and trimethylation of lysine 27 on histone H3 (H3K27me3) markers during late mouse retinal development by ChIP sequencing has been performed, and was used to categorize genes into several groups according to the modification pattern of H3K4 and H3K27 (1). A subset of genes specifically expressed in rod photoreceptors showed de novo accumulation of H3K4me2 (but not H3K27me3) on their locus, which correlates with transcriptional increases (1). In contrast, the distribution of H3K4me2 and H3K27me3 on genes widely expressed in the retina is not always associated with transcriptional levels (1). H3K27me3 was detected in the inner blastic layer at embryonic day (E) 16, and the signals were observed at the ganglion cell layer (GCL) and inner neuroblastic layer (INBL) at postnatal day (P) 0. In adults, GCL and inner nuclear layer (INL) nuclei stained strongly for the H3K27me3 marker (2). Popova et al. (1) also detected H3K27me3 in the GCL and INBL at E17.5, and H3K27me3 was maintained in some INL neurons at P1–P15 and in adults. Similarly, the spatial distribution of histone H3 trimethyl Lys4 and H3K4me2 was observed in the developing retina (1, 2). Chromatin compaction, the distribution of histone modification, and the location of RNA polymerase II in mouse rod photoreceptors were reported using cryopreparation methods, electron tomography, and immunogold labeling (3). Transcription occurs in the most decondensed and highly acetylated chromatin regions (3). Histone methyltransferase, G9a, which catalyzes dimethylation of H3K9, was enriched in the inner embryonic retina (2) and is important for the proper differentiation and survival of retinal progenitor cells (4). Histone demethylase Kdm5b contributed to rod photoreceptor homeostasis as a secondary node in the Nrl transcriptional hierarchy (5).

SI Materials and Methods

Mice. All animal experiments were approved by the Animal Care Committee of the Institute of Medical Science, University of Tokyo, and conducted in accordance with the Association for Research in Vision and Ophthalmology statement for the use of animals in ophthalmic and vision research. Institute of Cancer Research mice were obtained from the Japan SLC Company, and we checked to confirm that the mice were free of the Rd1 mutation. Therefore, the mice used in our work were free of retinal degeneration mutations.

DNA Construction. Full-length cDNAs encoding mouse *Bhlhb4* ORF were isolated by RT-PCR using mouse retinal RNA and subcloned into pCAG-internal ribosome entry site (IRES)-EGFP vector using the XhoI site. The shRNA vectors targeting mouse *Jmjd3* were constructed as described previously (6). Target sequences were 5′-aaggtgaaagggaaattccgaga (first) and 5′-aagtcttgtgattggctaaattt (second). BLAST analysis showed no homology between each target sequence and any other sequence in the human genome database. The efficiency of shRNA was examined using NIH 3T3 cells. We obtained similar results for major experiments using a second Jmjd3 shRNA. Full-length mouse *Jmjd3* in pCS2 was purchased from Addgene (catalog no. 17440, pCS2-Jmjd3-F), full-length *Neurod* was isolated by RT-PCR, and cloning of full-length *Chx10* has been described previously (7). They were subcloned into pCAG-IRES-EGFP vector using the XhoI site.

RT-PCR. Total RNA was purified from mouse retinas using RNeasy Plus Micro (QIAGEN), and cDNA was synthesized using SuperScript II (Life Technologies). Quantitative PCR was done by the SYBR Green-based method using a Roche LightCycler 1.5 apparatus and was analyzed by the second derivative maximum method for quantification (Roche Diagnostics). In accord with minimum information for publication of quantitative real-time PCR experiment guidelines (8), as an internal control, we examined expression levels of four housekeeping genes: Actb (beta-actin), Gapdh, Sdha, and Tbp. Then, the expression stability of these genes was analyzed according to geNorm methods. When we use cDNA of the retina at different developmental stages, the geNorm M value calculated with these four genes was greater than 0.5. When we calculated the geNorm M value with three genes (Gapdh, Sdha, and Tbp), we obtained a geNorm M value of less than 0.5. Among these genes, Gapdh and Sdha showed more stable expression than Tbp, and so we normalized results by the normalization factor (NF) value calculated using *Gapdh* and *Sdha*. In the case of shRNA for Jmjd3-expressing cell samples, the calculation using four genes showed a geNorm M value of less than 0.5 and the geNorm V2/3 value was less than 0.15. We normalized the results by using the NF value calculated with Actb and Tbp. For all RT-PCR analyses, we performed independent experiments three or four times, and values are shown with SDs in the relevant figures.

In Situ Hybridization of Jmjd3 and Utx. In situ hybridization was performed according to the standard protocol as previously described (9), using digoxigenin-labeled RNA probes. Because *Jmjd3* and *Utx* have high homology in the 5′ half, we used the 3′ half and the 3′ UTR of cDNA for probes. Control analysis was done using sense probes of the same region.

Retinal Explant, Electroporation, and BrdU Labeling. Retinal explants and in vitro electroporation were performed as described elsewhere (10, 11). The amount of plasmids used was 100 μg for one retina. The electroporated retinas were cultured at 34 °C on a chamber filter (Millicell; Millipore). For pulse labeling with BrdU to detect S-phase retinal progenitor cells, 1.5 μg/mL BrdU (Sigma–Aldrich) was present during the last 24 h of explant cultures. Incorporated BrdU was visualized as described previously (12).

Immunostaining. Immunostaining of frozen sections was done as described previously (10). Briefly, retinal explants were fixed with 4% (wt/vol) paraformaldehyde (PFA) for 10 min on ice, treated with 25% sucrose for 30 min, embedded in optimal cutting temperature compound (Miles), and sectioned (10-μm thickness) using a cryostat (CM3050S; Leica). For E14 samples, the head of embryos was fixed in 4% PFA for 30 min at room temperature and then replaced with sucrose as previously described (10). For E17 and more than E17 samples, eyes were enucleated and a hole was made by an 18-gauge needle; then, eyes were fixed in 4% (wt/vol) PFA for 10 min at room temperature followed by sucrose replacement. Appropriate secondary antibodies conjugated with Alexa Fluor dyes (Molecular Probes) were used to visualize signals. Samples were mounted in VectaShield (Vector Laboratories) and analyzed using a Zeiss Axio Vision 4.6 microscope.

Fluorescence-Activated Cell Sorting. Fractionation of Isl1-positive and Isl1-negative retinal cells was done as follows. Retinas at P9 were trypsinized and fixed by a 10-min incubation in formaldehyde (1% wt/vol), and glycine (125 mM final amount) was then added. After a 5-min incubation, the cells were permeabilized by a 5-min incubation on ice in PBS containing 0.1% Triton X-100 and 2% (wt/vol) BSA. Then, cells were stained with anti Isl1 antibody followed by staining with an appropriate second antibody. Sorting

was done using a MoFlo (DakoCytomation) or FACSAria (Becton Dickinson). Details of the sorting are shown in Fig. S5.

ChIP Assay. Mouse retinas cross-linked with 1% formaldehyde were suspended in 1% SDS lysis buffer and sonicated to shear genomic chromatin. The lysate was diluted and incubated for 1 d with antibody-bound Dynabeads-Protein G (Invitrogen). The beads were washed several times, and immune complexes were eluted. The eluate was incubated at 65 °C overnight to dissociate proteins from DNA and was treated with RNase A (37 °C for 30 min). The proteins were eliminated by digestion with proteinase K (Wako) at 55 °C for 1 h, and the DNA was purified with a QIAquick PCR purification kit (QIAGEN). The purified DNA was subjected to real-time PCR in a Roche Light Cycler 1.5 apparatus. The abundance of target genome DNA was normalized relative to that of input. For all ChIP experiments, independent experiments were done at least twice, and essentially the same results were obtained. One representative set of data is shown. Control IgG experiments gave only negligible values. For all ChIP experiments, independent experiments were done at least three times, and essentially the same results were obtained. Control IgG experiments gave only negligible values.

Statistics. P values [$^{**}P < 0.01$, $^{*}P < 0.05$, and $P > 0.05$ (not significant)] were calculated by the Student t test. Samples were from at least from three independent experiments.

SI List of Antibodies

Mouse Monoclonal Antibodies.

PKC (OP74; Calbiochem): rod-ON-BP cells (13), 1:200

PNR (PP-H7223-00; PPMX): rod photoreceptor, 1:500

Glutamine synthetase (GS; MAB302; Chemicon): Müller glia, 1:2,000

HuC/D (A-21272; Molecular Probes): amacrine cells (14), 1:500

Isl1 (39.4D5-c; DSHB): rod and cone-ON-BP and cholinergic amacrine cells (15, 16), 1:500

Ki67 (550609; BD Bioscience), 1:200

BrdU (11170376001; Roche), 1:20

Cyclin D3 (sc-182; Santa Cruz Biotechnology), 1:200

Ezh2 (3147; Cell Signaling), 1:200

Rabbit Polyclonal Antibodies.

Recoverin (AB5585; Chemicon): cone-OFF-BP cells (17), 1:6,000

GFP (632593; Clontech), 1:5,000

Phosphohistone H3 (06-570; Upstate), 1:500

Active caspase-3 (G748A; Promega), 1:250

H3K27me3 antibody (Abcam, ab6002), ChIP, 2μg

H3K27me3 antibody (Millipore, 07-449), 1:200

Histone H3 trimethyl Lys4 (H3K4me3) antibody (39159; Active Motif), ChIP, 2 μg

Jmjd3 (ab85392; Abcam), 1:200

Rat Monoclonal Antibody.

GFP (04404-84; Nacalai), 1:1,000

Sheep Polyclonal Antibody.

Chx10 (X1180P; Exalpha): a pan-bipolar marker, 1:500

Goat Polyclonal Antibodies.

Brn3 (C-13, sc-6026; Santa Cruz Biotechnology): ganglion cell, 1:200

Bhlhb5 (sc-6045; Santa Cruz Biotechnology): cone-OFF-BP cells and GABAergic amacrine cells (18), 1:2,000

Chicken Polyclonal Antibody.

GFP (ab13970; Abcam), 1:2,000

Secondary Antibodies.

Alexa Fluor 488 goat anti-chicken IgG (H+L) (A-11039; Invitrogen Molecular Probes), 1:2,000

Alexa Fluor 680 goat anti-mouse IgG (H+L) (A-21057; Invitrogen Molecular Probes), 1:2,000

Alexa Fluor 568 goat anti-rabbit IgG (H+L) (A-11011; Invitrogen Molecular Probes), 1:2,000

SI Primer Sequence List

Primer List for Construction (Cloning of Genes or in Situ Probes).

Jmjd3: 5′-ccgctcgagccggcatgcatcgggcagtggac-3′, 5′-tcccgcggccgctcatcgagacgtgctgg-3′

Bhlhb4: 5′-ccgctcgagcatggccgagctcaagtcgct-3′, 5′-ccgctcgagtcagggcttctcgccgcag-3′

Neurod: 5′-cccctcgagcaacaggaagtggaaacatg-3′, 5′-cccctcgagctaatcgtgaaagatggcatt-3′

Jmjd3 (for probe): 5′-gtcaatgaagcactgtcaggt-3′, 5′-agctgccaatagggtggaag-3′

Utx (for probe): 5′-gcttggaatgttggtccactt-3′, 5′-tggcataggagcagtactct-3′

Primer List for RT-PCR.

β-actin: 5′-ccaactgggacgacatggag-3′, 5′-tggtacgaccagaggcatacag-3′

Jmjd3: 5′-gtacagacccccggaacc-3′, 5′-tggtggagaaaaggcctaag-3′

Ezh2: 5′-cacctgttcccactgaggat-3′, 5′-agtgtgcagcccacaacc-3′

Chx10: 5′-ggagccatgttggactgaat-3′, 5′-gaagacatgccatcagtatgga-3′

Og9x: 5′-cagtcctgtggaggcatctc-3′, 5′-aactgcccgacactgaaagt-3′

Bhlhb5: 5′-ccttcagtgcggaagctct-3′, 5′-tgcctgcatgaggatgtagt-3′

Isl1: 5′-acgtgctttgttagggatgg-3′, 5′-tgaagcctatgctgcacttg-3′

Bhlhb4: 5′-aaaattacgccgaggtcctt-3′, 5′-tcacctcctgggatcttcc-3′

Vsx1: 5′-ggttgaaatgggttcttgct-3′, 5′-tgaggcaggagatcatgaaa-3′

Primers not listed have been published previously (9).

Primer List for ChIP Analysis. Primers for chip were designed around the transcription start site.

Bhlhb4: 5′-aggtcccctctgattggac-3′, 5′-gctctacctcccactcgtat-3′

Vsx1: 5′-agttgtaagctgccctgtgg-3′, 5′-cctgactggcacgtaggaat-3′

Chx10: 5′-ctagcctttgcgttcagacc-3′, 5′-agccaggtttggggttattc-3′

GS: 5′-acctctgtaccgttaaggaagc-3′, 5′-ttgcgttcttaagcgacctc-3′

Elavl3: 5′-cgagaggagaggacccatc-3′, 5′-cgagaggagaggacccatc-3′

Ink4a: 5′-gatggagcccggactacagaag-3′, 5′-ctgtttcaacgcccagctctc-3′

Abca4: 5′-gtgcccgcacttgtgtatttag-3′, 5′-tgattaaaggccgcgtttcc-3′

Tulp1:5′-gcttcccttcaatggttcagc-3′, 5′-agctaatctcggctcagcttc-3′

Lhx1: 5′-aacggacgtcttaccaaacc-3′, 5′-accgcgtttagaggatcagtg-3′

Olig2: 5′-attagccgggtgacatcagc-3′, 5′-gcgggaacaatgtgcttttc-3′

Neurod: 5′-acagatgggccactttcttc-3′, 5′-atatggtcttcccggtccag-3′

Primers not listed have been published previously (9).

1. Popova EY, et al. (2012) Stage and gene specific signatures defined by histones H3K4me2 and H3K27me3 accompany mammalian retina maturation in vivo. *PLoS ONE* 7(10):e46867.
2. Rao RC, et al. (2010) Dynamic patterns of histone lysine methylation in the developing retina. *Invest Ophthalmol Vis Sci* 51(12):6784–6792.
3. Kizilyaprak C, Spehner D, Devys D, Schultz P (2010) In vivo chromatin organization of mouse rod photoreceptors correlates with histone modifications. *PLoS ONE* 5(6):e11039.
4. Katoh K, Yamazaki R, Onishi A, Sanuki R, Furukawa T (2012) G9a histone methyltransferase activity in retinal progenitors is essential for proper differentiation and survival of mouse retinal cells. *J Neurosci* 32(49):17658–17670.
5. Hao H, et al. (2012) Transcriptional regulation of rod photoreceptor homeostasis revealed by in vivo NRL targetome analysis. *PLoS Genet* 8(4):e1002649.
6. Satoh S, et al. (2009) The spatial patterning of mouse cone opsin expression is regulated by bone morphogenetic protein signaling through downstream effector COUP-TF nuclear receptors. *J Neurosci* 29(40):12401–12411.
7. Tabata Y, et al. (2004) Specification of the retinal fate of mouse embryonic stem cells by ectopic expression of Rx/rax, a homeobox gene. *Mol Cell Biol* 24(10):4513–4521.
8. Bustin SA, et al. (2009) The MIQE guidelines: Minimum information for publication of quantitative real-time PCR experiments. *Clin Chem* 55(4):611–622.
9. Koso H, et al. (2008) CD138/syndecan-1 and SSEA-1 mark distinct populations of developing ciliary epithelium that are regulated differentially by Wnt signal. *Stem Cells* 26(12):3162–3171.
10. Iida A, Shinoe T, Baba Y, Mano H, Watanabe S (2011) Dicer plays essential roles for retinal development by regulation of survival and differentiation. *Invest Ophthalmol Vis Sci* 52(6):3008–3017.
11. Ouchi Y, Tabata Y, Arai K, Watanabe S (2005) Negative regulation of retinal-neurite extension by β-catenin signaling pathway. *J Cell Sci* 118(Pt 19):4473–4483.
12. Usui A, et al. (2013) The early retinal progenitor-expressed gene Sox11 regulates the timing of the differentiation of retinal cells. *Development* 140(4):740–750.
13. Haverkamp S, Ghosh KK, Hirano AA, Wässle H (2003) Immunocytochemical description of five bipolar cell types of the mouse retina. *J Comp Neurol* 455(4):463–476.
14. Ekström P, Johansson K (2003) Differentiation of ganglion cells and amacrine cells in the rat retina: Correlation with expression of HuC/D and GAP-43 proteins. *Brain Res Dev Brain Res* 145(1):1–8.
15. Galli-Resta L, Resta G, Tan SS, Reese BE (1997) Mosaics of islet-1-expressing amacrine cells assembled by short-range cellular interactions. *J Neurosci* 17(20):7831–7838.
16. Elshatory Y, Deng M, Xie X, Gan L (2007) Expression of the LIM-homeodomain protein Isl1 in the developing and mature mouse retina. *J Comp Neurol* 503(1):182–197.
17. Haverkamp S, Wässle H (2000) Immunocytochemical analysis of the mouse retina. *J Comp Neurol* 424(1):1–23.
18. Feng L, et al. (2006) Requirement for Bhlhb5 in the specification of amacrine and cone bipolar subtypes in mouse retina. *Development* 133(24):4815–4825.

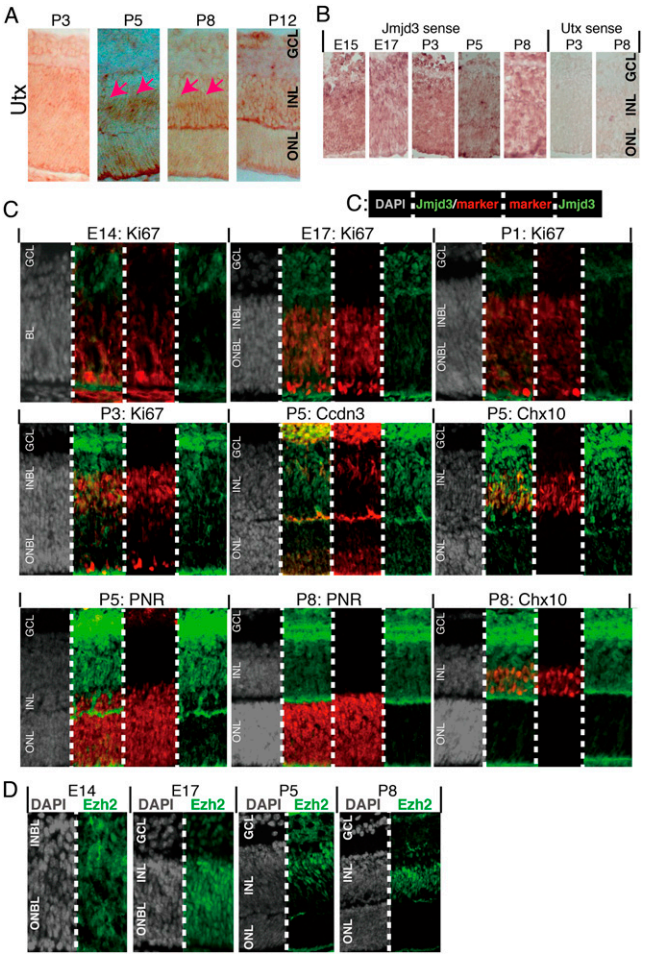

Fig. S1. Expression of Utx and Jmjd3 in developing retina. In situ hybridization (*A* and *B*) or immunostaining (*C* and *D*) of *Utx* (*A*), Jmjd3 (*C*), and Ezh2 (*D*) in developing mouse retina. Mouse retinas at the indicated developmental stage were frozen-sectioned, and in situ hybridization or immunostaining was done. Pink arrows in *A* indicate Utx signals in INL. (*B*) Sense control of *Jmjd3* and *Utx* in situ hybridization is shown. (*C*) Double staining with indicated antibodies is shown. BL, blastic layer; ONBL, outer neuroblastic layer; ONL, outer nuclear layer.

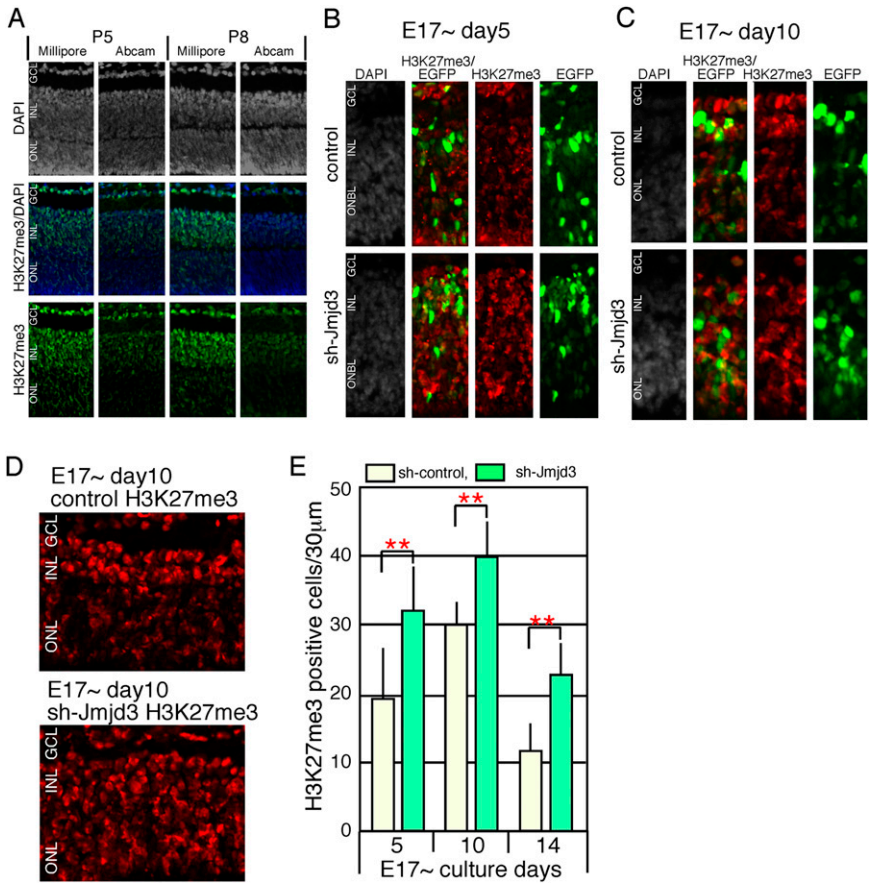

Fig. S2. Immunostaining of H3K27me3 using retinal sections. (*A*) Immunostaining of H3K27me3 using two different antibodies in the retina at P5 or P8 was done. (*B–D*) Immunostaining patterns of H3K27me3 (Millipore antibody) using retinal sections expressing short hairpin (sh)-control or shRNA for *Jmjd3* (sh-Jmjd3) are shown. Plasmids were electroporated into the retina at E17, and retinas were cultured for 5 d (*B*) or 10 d (*C* and *D*). (*D*) Larger area of anti-H3K27me3 staining pattern as shown in *C*. (*E*) H3K27me3-positive cells in sh-control or sh-Jmjd3–expressing retina. More than five sections from three independent samples were counted, and values with SDs are shown. $^{**}P < 0.01$ was calculated by the Student *t* test.

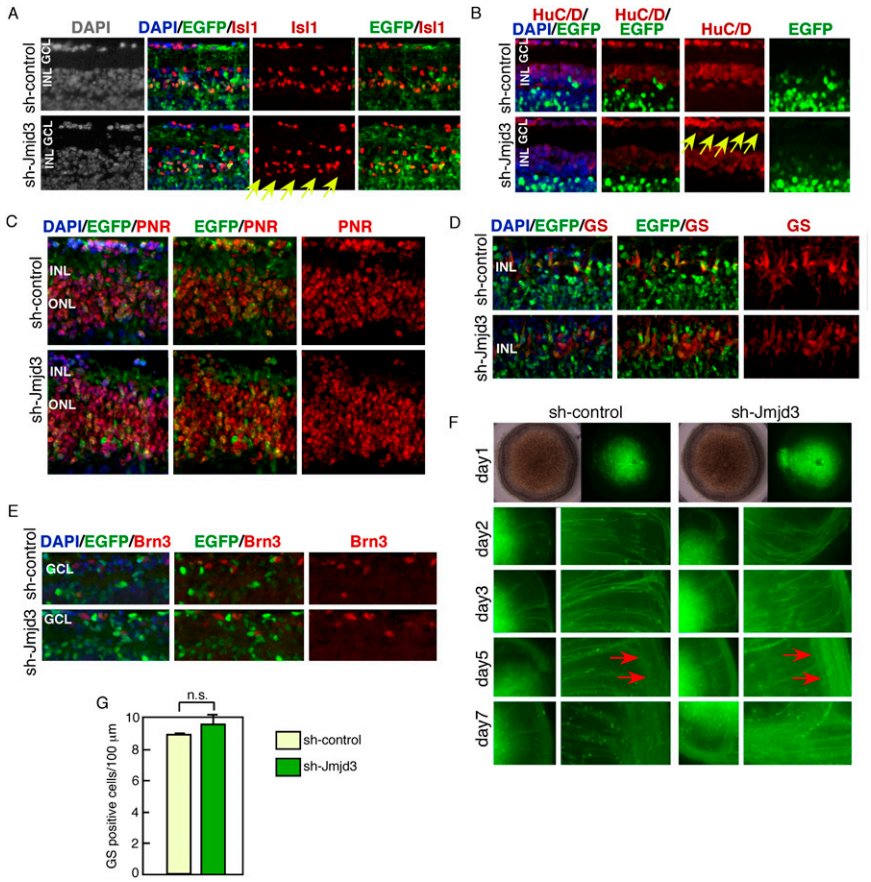

Fig. S3. Differentiation of retinal cells after transfection of sh-Jmjd3. Retina at E17 (*A–D*) or E14 (*E*) was transfected with control or sh-Jmjd3 and cultured for 2 wk (*A–D*) or 7 d (*E*). The retina was frozen-sectioned and immunostained with anti-Isl1 (*A*), anti-HuC/D (*B*), anti-PNR (C), anti-GS (*D*), and anti-Brn3 (*E*). Yellow arrows in *A* indicate Isl1-positive ON-BP, and yellow arrows in *B* indicate displaced amacrine cells. (*F*) Retina at E14 was transfected with control or sh-Jmjd3 and cultured as explant cultures. Photos of the whole-mount retina were taken on the indicated days. Enlargements (*Right*) of a portion of the photos (*Left*) are shown. Arrows indicate neurite around the explants. (*G*) Retina at E14 was transfected with control or sh-Jmjd3 and cultured for 7 d. The number of GS-positive cells was counted in more than four independent panels for each sample, and average values with SDs are shown. n.s., not significant.

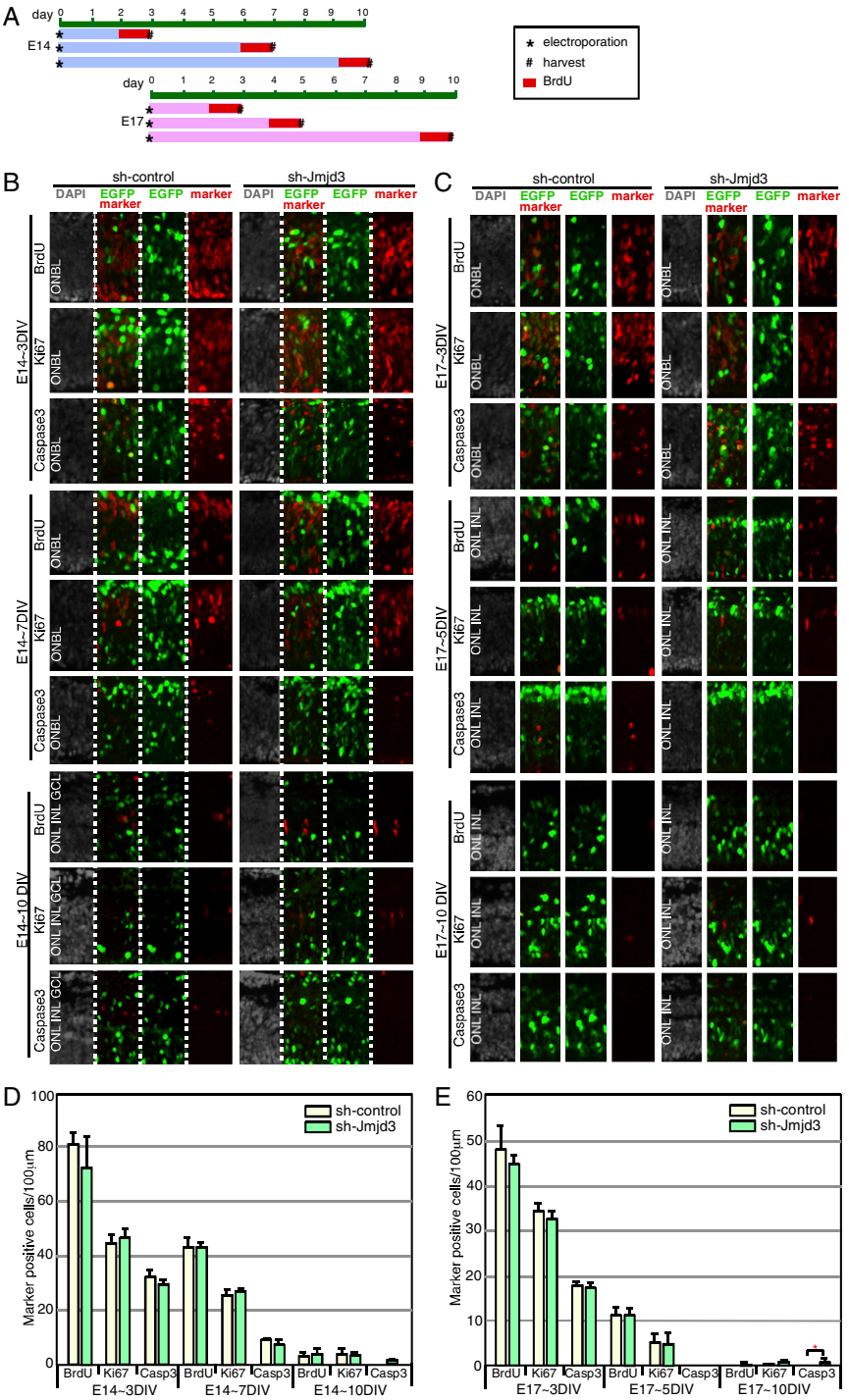

Fig. S4. Effects of sh-Jmjd3 for proliferation of retinal progenitor cells. (*A*) Schematic representation of experimental design. Plasmids encoding sh-Jmjd3 or sh-control with CAG-EGFP were introduced into the retina at E14 (*B* and *D*) or E17 (*C* and *E*), and the retina was cultured for the indicated number of days as retinal explants. BrdU was present in the culture medium during the last 24 h of culture. Explants were harvested, proliferation was examined by immunostaining of incorporated BrdU and Ki67 proliferation antigen, and apoptotic cells were examined by immunostaining of active caspase-3. More than five sections from three independent samples were counted, and values with SDs are shown in *D* and *E*. *$P < 0.05$ and $P > 0.05$ (no symbol) were calculated the by Student *t* test. DIV, days in vitro.

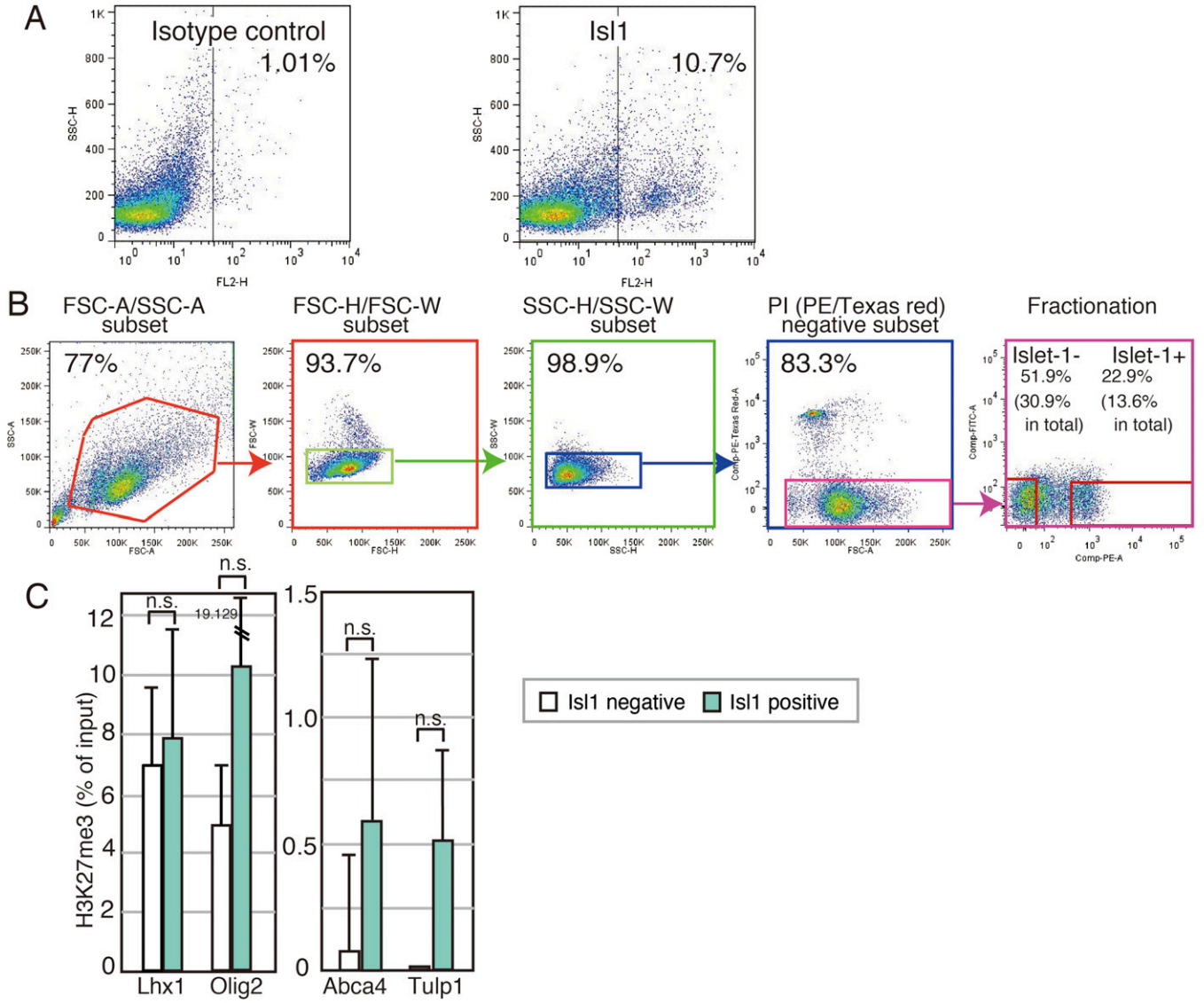

Fig. S5. ChIP analysis and fluorescence-activated cell sorting (FACS) patterns of Isl1-stained retinas. (*A* and *B*) Retinas at P9 were stained with anti-Isl1 antibody. (*A*) FACS pattern of retina stained with isotype control Ig or anti-Isl1 antibody examined by FACS. (*B*) FACS pattern of separation of retina stained with anti-Isl1 antibody. Cell sorting was done using FSC/SSC gating, and duplicated cells were then excluded by FSC-W, followed by SSC-W window. FSC, forward scatter; SSC, side scatter; A, area; H, height; W, width. Then, dead cells were excluded by phycoerythrin (PE)-positive cells, and Isl1-positive and Isl1-negative cells were purified. (*C*) H3K27me3 levels of Isl1-positive and Isl1-negative cells. H3K27me3 modification of gene loci in purified Isl1-positive or Isl1-negative cells was examined by ChIP analysis.

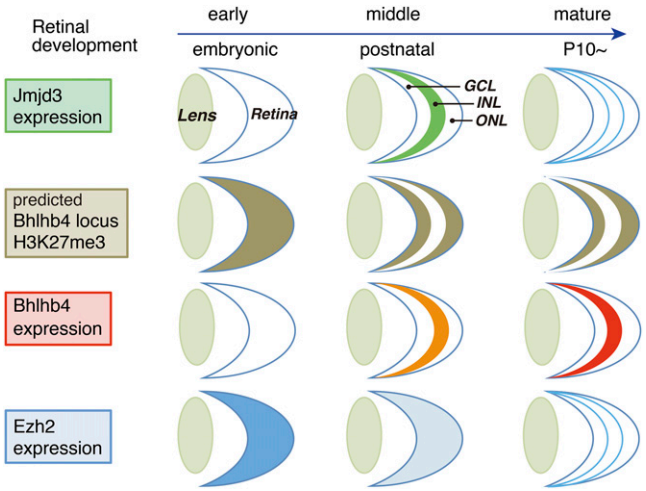

Fig. S6. Schematic diagram of expression pattern of Jmjd3/Ezh2 and Bhlhb4. Spatial expression patterns of Jmjd3 (*Top*) and Ezh2 (*Bottom*) during retinal development are schematically shown in upper and lower columns. (*Middle* two rows) Expression pattern of Bhlhb4 and predicted H3K27me markers in the *Bhlhb4* locus are schematically shown.